IOP Publishing Phys. Scr. 99 (2024) 115102 https://doi.org/10.1088/1402-4896/ad7f11

Physica Scripta

OPEN ACCESS

RECEIVED
29 July 2024

REVISED
17 September 2024

ACCEPTED FOR PUBLICATION
24 September 2024

PUBLISHED
3 October 2024

PAPER

The impact of quantum correlations on parameter estimation in a spin reservoir

Ali Raza Mirza* and **Jim Al-Khalili**

Department of Physics, University of Surrey, GU2 7XH, Guildford, United Kingdom

* Author to whom any correspondence should be addressed.

E-mail: a.r.mirza@surrey.ac.uk

Keywords: parameter estimation, spin-spin model, initial correlations, quantum Fisher information

Abstract

We study the impact of quantum correlations existing within the system-environment thermal equilibrium state while estimating the parameters of the spin reservoir. By employing various physical situations of interest, we present results for the reservoir temperature and its coupling strength with the central two-level system. The central system (probe) interacts with the bunch of randomly oriented spin systems and attains a thermal equilibrium state. We consider a projective measurement which prepares the probe's initial state, and then the global system (probe and reservoir) evolves unitarily. The reduced density operator encapsulates the information about the spin reservoir which can be extracted by doing measurements on the probe. The precision of such measurement is quantified by quantum Fisher information. We repeat this process if the probe-reservoir initial state is not correlated (product state). We compare the estimation results for both with and without the outturn of initial correlations. In the temperature estimation case, our results are promising as one can significantly improve the accuracy of the estimates by including the effect of initial correlations. A similar trend prevails in the case of coupling strength estimation especially at low temperatures.

1. Introduction

Open quantum systems have garnered immense attention due to their fundamental role in the advancement of modern quantum technologies [1]. To properly understand quantum dynamics, it is important to scrutinize the impact of the environment, as every quantum system interacts with its surrounding environment in some way, leading to decoherence [2, 3]. To comprehend this effect, it is essential to learn about the environmental parameters such as its temperature and the coupling strength. A useful approach involves using a quantum probe (a small controllable quantum system) undergoing pure dephasing [4–17]. The quantum probe is allowed to interact with its surrounding environment (spin reservoir) until they both reach an equilibrium state (probe-environment correlated state) [18]. Subsequently, a measurement on the probe results in the desired initial state and then this whole system evolves under the total unitary operator. Unfortunately, studying the dynamics of such a big (probe-environment) system is challenging due to the environment's many degrees of freedom. One possible to tackle this is to utilize exactly solvable models [19, 20]. Once reduced dynamics are obtained, the various properties of the environment can be learned by performing a measurement on the probe. This also enables one to estimate environment parameters. Theoretically, a very useful estimation tool is to derive quantum Fisher information (QFI), which quantifies the ultimate precision in the measurement [21–25]. According to the Cramér-Rao bound (CRB), the uncertainty in any estimator x is bounded by the reciprocal of the Fisher information $F(x)$, that is, $\Delta x \geqslant 1/F(x)$. Thus, to minimize error in the measurement, $F(x)$ has to be maximized.

To date, many efforts have been made to estimate environmental parameters. This goal is typically achieved by initially setting the probe and environment in a product state. Recent works, such as in [14, 15], demonstrate that the environment remains at thermal equilibrium throughout, and the quantum correlations developed after the initial state preparation process are wielded to extract the environmental information. Single-qubit and

two-qubit quantum systems have been utilized as a probe to estimate the cutoff frequency of the harmonic oscillator reservoir and the spectral characterization of classical noisy environments [4, 5, 11, 26]. These attempts disregard the quantum correlations in the probe-environment equilibrium state and employ quantum Fisher information formalism. On the other hand, improvements in the joint estimation of nonlinear coupling and nonlinearity order have been reported by squeezing quantum probes connected to nonlinear media [27]. Conversely, quantum metrology employs quantum resources to enhance the sensitivity of both single and multiple-phase estimations [28]. However, these findings are debatable, specifically at strong reservoir coupling where the impact of initial correlations is quite significant. The importance of initial correlations present before state preparation has often been looked over [29–40]. More recently, [20, 41] looked into the effects of these correlations in the estimation using the QFI approach. Taking the basic seed of this idea, we extend our study to explore the impact of correlations within a spin reservoir.

We begin with formulating the reduced dynamics of the probe which is coupled to the spin reservoir. For that, we first prepare our probe (at thermal equilibrium with the reservoir) in the state 'up' along the x-axis through a projective measurement at $t = 0$. Subsequently, the probe undergoes decoherence and dissipation via environmental interaction. To obtain reduced dynamics, a partial trace is performed to average out the effect of the environment. In the reduced density matrix, both diagonal and off-diagonal elements evolve with time. More importantly, dissipation and decoherence rates have been modified due to the correlations that existed in the Gibbs state. Diagonalization of this density matrix enables us to derive the expression of QFI, which is a function of the probe-environment interaction time as well as other parameters. The idea here is to pick up an interaction time such that QFI is maximum. We conclusively show that the corresponding maximum QFI can be greater than the QFI obtained disregarding initial correlations. Our findings emphasize that when the coupling is strong and the temperature is low, initial correlations play a remarkable role in improving the accuracy of our measurements.

This paper is organised as follows; In section 2, we present the scheme of state preparation. Section 3 details the spin-spin model and its dynamics for the case of the initial correlation, while the dynamics without the initial correlations have been put in appendix section 6. In the next section 4, we derive the formulae of quantum Fisher information for both with and without initial correlations cases and present the estimation results for the temperature and coupling strength. Then we have the main part of this paper where the estimation results for temperature and coupling strength are shown. Finally, we conclude this paper in section 5.

2. Preparation of initial state

The usual choice of probe-environment initial state is the product state $\rho^{u}_{\rm tot} = \rho_S \otimes \rho_E$. To prepare the probe in state $|\varphi\rangle$, we perform a selective measurement at $t = 0$ using the projection operator $|\varphi\rangle\langle\varphi|$. This gives

$$\rho^{u}_{\rm tot}(0) = |\varphi\rangle\langle\varphi| \otimes \frac{\mathrm{Exp}\{-\beta H_E\}}{Z_E}, \tag{1}$$

where, $Z_E = \mathrm{Tr}_E[\mathrm{e}^{-\beta H_E}]$ is called partition function of the environment only. This state is regarded as a product state of the probe and its environment. As superscript 'u' suggests, this state is referred to as the 'uncorrelated state' as the probe-environment interaction before the state preparation process has been ignored. However, in the natural probe-environment thermal equilibrium state, quantum correlations are present. Thus, one can perceive the idea of initial correlations by imagining that at $t < 0$, our probe has interacted with the environment till it reaches the canonical Gibbs state. The joint thermal equilibrium state is now $\rho_{\rm th} = e^{-\beta H_{\rm tot}}/Z_{\rm tot}$, with $Z_{\rm tot} = \mathrm{Tr}_{S,E}[\mathrm{e}^{-\beta H_{\rm tot}}]$ and $H_{\rm tot} = H_S + H_{SE} + H_E$. Due to the presence of correlations, this state cannot be expressed as a tensor product of the probe and the environment. If we chose a probe with a large energy bais as compared to the tunnelling amplitude, that is $\varepsilon >> \Delta$, the thermal equilibrium state of the probe will be approximately 'down' along the z-axis. This orientation can easily be proved by invoking Born's postulate. A projective measurement on such a state entails the total probe-environment state

$$\rho^{c}_{\rm tot}(0) = |\varphi\rangle\langle\varphi| \otimes \frac{\langle\varphi|\,\mathrm{Exp}\{-\beta H_{\rm tot}\}\,|\varphi\rangle}{Z_{\rm tot}}, \tag{2}$$

which is still a product state as the projective measurement has lifted the probe-environment correlations. Now the superscript 'c' denotes the 'correlated initial state'. Now the total probe-environment state is no longer in equilibrium. It is important to note that the initial environment state depends on the H_{SE} as well as the method of the probe's state preparation. It is obvious that if the probe-environment coupling is sufficiently small, then the state equation (2) will be the same as that in equation (1). In other words, for weak coupling, the impact of the initial correlations is unimportant. Furthermore, the state preparation process also influences the environment state due to the presence of correlations. Thus, the outturn of correlations is further dependent on how the probe's state is prepared. In this paper, we only deal with the projective measurement that prepares our probe in

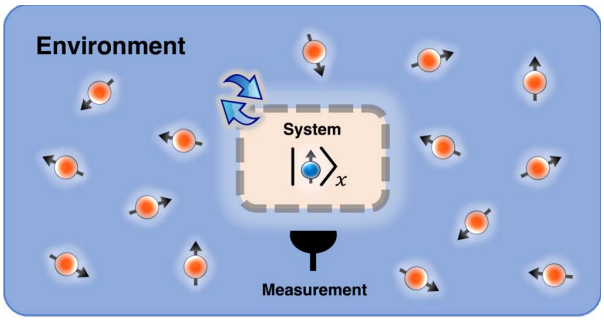

Figure 1. A spin-spin model where a central spin (probe) is coupled to the N environment spins. A projective measurement prepares the probe in the state 'up' along the x-axis.

the pure state. We set our projector such that the probe's initial state is 'up' along the x-axis shown in figure 1, for both with or without the initial correlations cases. This initial state corresponds to the Bloch vector components at $t = 0$ to be $a_x^c(0) = 1$, $a_y^c(0) = 0$, $a_z^c(0) = 0$ for the case of correlations and $a_x^u(0) = 1$, $a_y^u(0) = 0$, $a_z^u(0) = 0$ for the case of without initial correlations. Any other measurement may enhance the obtained Fisher information however, In this paper, we restrict ourselves only to the projective measurement.

3. The model and its dynamics

Our objective is to estimate parameters that characterize the environment of our quantum system. We use a spin-spin model where a central spin (probe) interacts with the collection of spins (environment). According to this model

$$H_S = \frac{\epsilon}{2}\sigma_z + \frac{\Delta}{2}\sigma_x, \tag{3a}$$

$$H_E = \sum_{i=1}^{N}\left(\frac{\omega_i}{2}\sigma_z^{(i)} + \chi_i\sigma_z^{(i)}\sigma_z^{(i+1)}\right), \tag{3b}$$

$$H_{SE} = \frac{1}{2}\sigma_z \otimes g\sum_{i=1}^{N}\sigma_z^{(i)}, \tag{3c}$$

here $\sigma_{x,y,z}$ are the Pauli spin operators while ϵ and Δ symbolize the energy bias and the tunnelling amplitude of the probe respectively. Similarly, ω_i represents the energy bias of the ith spin belonging to the environment. We incorporate the inter-spin interaction between the environmental spins via the term $\sum_{i=1}^{N}\sigma_z^{(i)}\sigma_z^{(i+1)}\chi_i$ where χ_i characterises the nearest neighbour interaction. The probe interacts with the environmental spins via interaction Hamiltonian H_{SE}, where g is the probe-environment coupling strength which is assumed to be the same for each environmental spins. We write $H_{SE} = S \otimes E$, where S stands for the system (probe) operator and E stands for the environment (spin reservoir) operator. Also, we take $|e\rangle = |e_1\rangle|e_2\rangle|e_3\rangle...|e_N\rangle$ be the eigenvectors of the environment operator, E. with $e_i = 0, 1$. The states $|0\rangle$ and $|1\rangle$ 'up' and 'down' state respectively. Also, $[H_E, E] = 0$, thus we have

$$g\sum_{i=1}^{N}\sigma_z^{(i)}|e\rangle = \tilde{\zeta}_N|e\rangle; \qquad \sum_{i=1}^{N}\omega_i\sigma_z^{(i)}|e\rangle = \omega_N|e\rangle; \qquad \sum_{i=1}^{N}\chi_i\sigma_z^{(i)}\sigma_z^{(i+1)}|e\rangle = \alpha_N|e\rangle, \tag{4}$$

with $\omega_N = \sum_{i=1}^{N}(-1)^{e_i}\omega_i$ and $\alpha_N = \sum_{i=1}^{N}\chi_i(-1)^{e_i}(-1)^{e_{i+1}}$. with $\tilde{\zeta}_N = g\sum_{i=1}^{N}(-1)^{e_i}$. We assume all spins are coupled to the central spin with equal strength, terms having tilde overhead, meaning that they are a function of coupling strength g. Here, we only show the dynamics of the probe if correlations are incorporated whereas the dynamics of no correlations case has been given in the appendix section 6. Dynamics can be obtained by performing a partial trace over the environment, that is, $\rho_c(t) = \mathrm{Tr}_E[\mathrm{U(t)}\rho_{\mathrm{tot}}^c(0)\mathrm{U}^\dagger(\mathrm{t})]$, where the unitary operator is calculated as

$$U(t) = \sum_N \mathrm{Exp}\left\{-i\frac{\omega_N}{2}t\right\}\mathrm{Exp}\left\{-i\alpha_N t\right\}\mathrm{Exp}\left\{-i\widetilde{H}_S^N t\right\}|e\rangle\langle e| = \sum_N U_N(t)|e\rangle\langle e|, \tag{5}$$

where $U_N(t) = \mathrm{Exp}\left\{-i\frac{\omega_N}{2}t\right\}\mathrm{Exp}\left\{-i\alpha_N t\right\}\mathrm{Exp}\left\{-i\widetilde{H}_S^N t\right\}$ only acting on the system's Hilbert space, $\widetilde{H}_S^N \equiv \frac{\tilde{\epsilon}_N}{2}\sigma_z + \frac{\Delta}{2}\sigma_x$ shifted Hamiltonian with $\tilde{\epsilon}_N = \epsilon + g\sum_{i=1}^{N}(-1)^{e_i} \equiv \epsilon + \tilde{\zeta}_N$. After some algebraic manipulations, we obtain a reduced density matrix

$$\rho_c(t) = \frac{1}{Z_{\rm tot}}\sum_N Q_n c_N U_N(t)|\varphi\rangle\langle\varphi| U_n^\dagger(t) = \frac{1}{2}\begin{pmatrix} 1 + a_z^c(t) & e^{-\Gamma_c(t)}e^{-i\Omega_c(t)} \\ e^{-\Gamma_c(t)}e^{i\Omega_c(t)} & 1 - a_z^c(t)\end{pmatrix}, \tag{6}$$

with $\Omega_c(t) = \arctan\left[\frac{a_y^c(t)}{a_x^c(t)}\right]$, and the decoherence rate $\Gamma_c(t) = -\frac{1}{2}\ln|\{a_x^c(t)\}^2 + \{a_y^c(t)\}^2|$. The evolution of the corresponding Bloch vector components can be written in general form as $a_i^c(t) = \Lambda_{ix}^c(t)a_i^c(0)$, with $i = x, y, z$, where

$$\Lambda_{xx}^c(t) = \sum_N \frac{Q_N c_N}{4Z_{\rm tot}\eta_N^2}\{\Delta^2 + \eta_N^2\cos(2\eta_N t)\};$$
$$\Lambda_{yx}^c(t) = \sum_N \frac{Q_N c_N \varepsilon_N}{2Z_{\rm tot}\eta_N}\sin(2\eta_N t);$$
$$\Lambda_{zx}^c(t) = \sum_N \frac{Q_N c_N \tilde{\epsilon}_N \Delta}{2Z_{\rm tot}\eta_N^2}\sin^2(\eta_N t).$$

Here $Z_{\rm tot} = \sum_N Q_N c_N$ with $Q_N = \cosh(\beta\eta_N) - (1/\eta_N)\cosh(\beta\eta_N)\langle\varphi|\widetilde{H}_S^N|\varphi\rangle$, $\eta_N = (1/2)\sqrt{\tilde{\epsilon}_N^2 + \Delta^2}$, and $c_N = e^{-\beta\frac{\omega_N}{2}}e^{-\beta\alpha_N}$. For convenience, we work in the dimensionless units, where every energy parameter is expressed in terms of ε. Thus, we have set $\hbar = k_B = 1$, during calculations and throughout the paper. Eigenvalues of $\rho_c(t)$ [equation (6)] calculated as $\rho_1(t) = \frac{1}{2}[1 + A_c(t)]$, $\rho_2(t) = \frac{1}{2}[1 - A_c(t)]$ with $A_c(t) = \sqrt{\{a_x^c(t)\}^2 + \{a_y^c(t)\}^2 + \{a_z^c(t)\}^2}$. Corresponding eigenvectors are

$$|v_1^c(t)\rangle = \sqrt{\frac{A_c(t) + a_z^c(t)}{2A_c(t)}}\,|\downarrow\rangle_z - e^{-i\Omega_c(t)}\sqrt{\frac{A_c(t) - a_z^c(t)}{2A_c(t)}}\,|\uparrow\rangle_z, \tag{7a}$$

$$|v_2^c(t)\rangle = \sqrt{\frac{A_c(t) - a_z^c(t)}{2A_c(t)}}\,|\downarrow\rangle_z + e^{-i\Omega_c(t)}\sqrt{\frac{A_c(t) + a_z^c(t)}{2A_c(t)}}\,|\uparrow\rangle_z, \tag{7b}$$

where $|\uparrow\rangle_z$ and $|\downarrow\rangle_z$ are eigenstates of σ_z with eigenvalues $+1$ and -1 respectively. If we disregard initial correlations, we obtain an analogous expression of the system density matrix $\rho_u(t)$ given by equation (11). For associated details, the reader is referred to the appendix section 6.

4. Parameter estimation

As a first step towards the parameter estimation, we need to derive the formula for the quantum Fisher information for the probe (a two-level quantum system) under consideration.

4.1. Derivation of quantum Fisher Information

To quantify the accuracy in any estimator x, the general formula for the quantum Fisher information is given by [11]

$$F(x) = \sum_{n=1}^{2}\frac{(\rho'_n)^2}{\rho_n} + 2\sum_{n\neq m}\frac{(\rho_n - \rho_m)^2}{\rho_n + \rho_m}|\langle v_m|v'_n\rangle^2|, \tag{8}$$

where $\rho_{m,n}$ and $v_{m,n}$ being eigenvalues and eigenvectors of any density matrix respectively. The superscript prime (') denotes the derivative with-respect-to x (in our case this can be temperature, T, or the coupling strength, g. Since we have diagonalized the $\rho_c(t)$, then, after some algebra we arrive at

$$F_c(x) = \frac{(\Gamma'_c - a_z^c(a_z^c)'e^{2\Gamma_c})^2}{f_c(e^{2\Gamma_c} - f_c)} + \frac{((a_z^c)' + a_z^c\Gamma'_c)^2}{f_c} + \frac{(\Omega'_c)^2}{e^{2\Gamma_c}}, \tag{9}$$

with $f_c = 1 + (a_z^c)^2e^{2\Gamma_c}$. In the chosen probe-environment model, both diagonal and off-diagonal entries evolve. Therefore, we can see the Fisher information also depends on the time-dependent factor $a_z^c(t)$. However, in the pure-dephasing case (where only off-diagonal entries evolve), $a_z^c = 0$, and $f_c = 1$, hence we recover the Fisher information given in [42], and benchmark our calculations. The analogous expression for QFI, when disregarding the initial correlations, can be written as

$$F_u(x) = \frac{(\Gamma'_u - a_z^u(a_z^u)'e^{2\Gamma_u})^2}{f_u(e^{2\Gamma_u} - f_u)} + \frac{((a_z^u)' + a_z^u\Gamma'_u)^2}{f_u} + \frac{(\Omega'_u)^2}{e^{2\Gamma_u}}, \tag{10}$$

with $f^u = 1 + (a_z^u)^2e^{2\Gamma_u}$, $\Omega_u(t) = \arctan\left[\frac{a_y^u(t)}{a_x^u(t)}\right]$, and $\Gamma_u(t) = -\frac{1}{2}\ln|\{a_x^u(t)\}^2 + \{a_y^u(t)\}^2|$. Now $a_x^u(t)$, $a_y^u(t)$, $a_z^u(t)$ are the components of the Bloch vector but for the case of uncorrelated initial state.

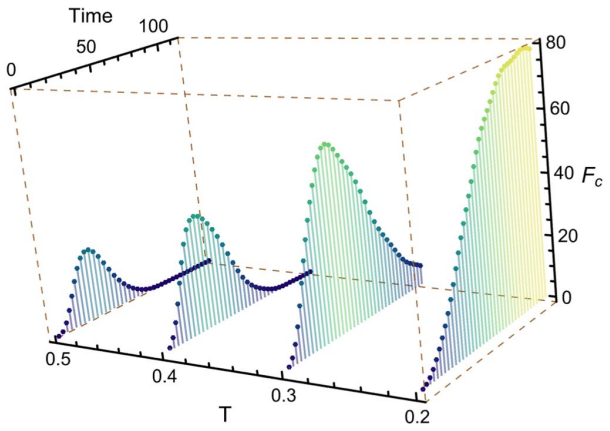

Figure 2. Here we show the behaviour of the QFI for certain values of temperature T as a function of time, incorporating the initial correlations, where F_c denoted the QFI for the case of the correlations. Peaks of F_c represent the ultimate precision while estimating the temperature of the environment. We have considered the number of environmental spins to be $N = 50$, with coupling strength $g = 0.01$, and inter-spin interaction $\chi = 0$. The rest of the parameters are $\omega_i = 1, \varepsilon = 2$ and $\Delta = 1$.

4.2. Estimating temperature of the environment

With the expressions for quantum Fisher information at hand, with and without the initial correlations, we now move to estimate the temperature. As mentioned earlier in the introduction section, quantum Fisher information is linked with the CRB; we can maximise the precision of the estimate by maximising QFI. Therefore our goal here is to maximize the QFI equation (9) over the interaction time. As a first example, we consider estimating the environment temperature. All we need to do is to calculate partial derivatives with-respect-to temperature T using equation (9). We demonstrate the optimization scheme in 3D in figure 2 where the behaviour of QFI has been plotted as a function of interaction time for certain values of temperature. We have considered the number of spins in the environment $N = 50$ which are all assumed to be at a distance from each other such that inter-spin interactions can be ignored. Peak values of QFI are called optimal values at chosen temperatures. The height of peaks quantifies the accuracy associated with the measurement outcome, which seems to be descending. Their shapes make sense because the quantum state is very sensitive to the temperature. As the temperature is raised, the decoherence process speeds up, we start losing the benefits of quantum properties, quantum sensing is one of them which we are addressing in this paper. This figure serves as an overview of how quantum Fisher information is optimized in our later results.

We aim to improve the precision of the temperature estimates, We plot QFI as a function of time for each value of T for both the cases with and without initial correlations, using equation (9) and equation (10) respectively. The role of initial correlation is captured by the Q_n. First, we consider probe-environment coupling to be weak where the effect of correlations is minimal [17, 20, 34]. This leads us to the negligible impact on the accuracy of our measurement estimates. Exactly the same trend is illustrated in figure 3(a) where we have taken $g = 0.01$. We note that if correlations are discarded, there is minimal effect on the precision associated with the temperature measurement. The strong overlap between the two curves is evidence. This is because the contribution of the system Hamiltonian, H_S dominates the interaction Hamiltonian, H_{SE}. However, as interaction strength increases, the impact of correlations is anticipated to be significant (as depicted in figure 3(b)). Here, the solid, dashed and dot-dashed curves denote QFI including correlations, while curves made up of circles, squares, and triangles signify QFI without initial correlations. At least two comments can be made regarding this result. First, at intermediate coupling strength $g = 0.05$, a slight improvement in the precision can be realised for the smaller values of temperatures, but this scenario noticeably changes as we move into the strong coupling regime where curves due to correlations are higher than elevated than those without correlations. Therefore, precision can be significantly improved via initial correlations in the case of strong coupling.

Next, we look into the role of the size of the environment, (that is, the number of spins present in our environment). Before proceeding, we generate a standard plot for $N = 10$ in both the cases with (black-solid) and without (black-dotted) correlations to show better comparison with the larger environment where $N = 15$ (figure 4(a)) and with $\chi = 0.1$ (figure 4(b)). Since a large environment speeds up the decoherence process, we might expect a decrease in QFI as the number of spins in the environment increases. However, the results shown in figure 4(a) show that the Fisher information is larger $N = 15$ than those for which $N = 10$. This implies that a larger environment is favourable for quantum measurements as long as decoherence has not gone through. But

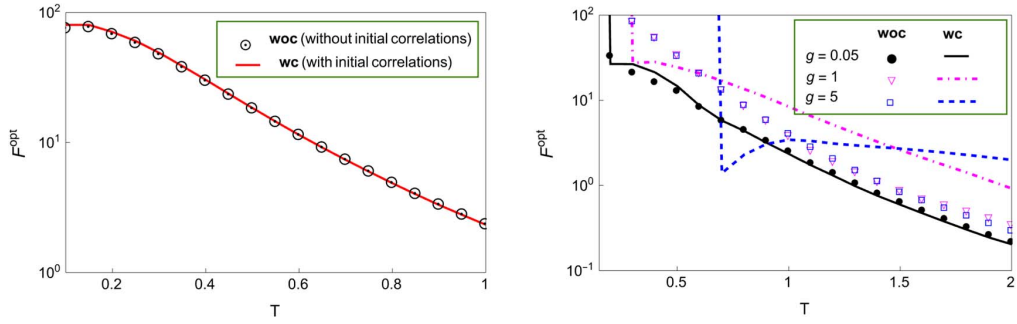

(a) $g = 0.01$ **(b)** $g = 0.05, 1, 5$

Figure 3. Figures show the behaviour of the optimized QFI (F^{opt}) estimating environment temperature with and without initial correlations. 3(a) considers probe-environment coupling strength $g = 0.01$ while 3(b) consider various strengths $g = 0.05$(black), 1(magenta), 5(blue). Other probe-environment parameters are selfsame as in figure 2.

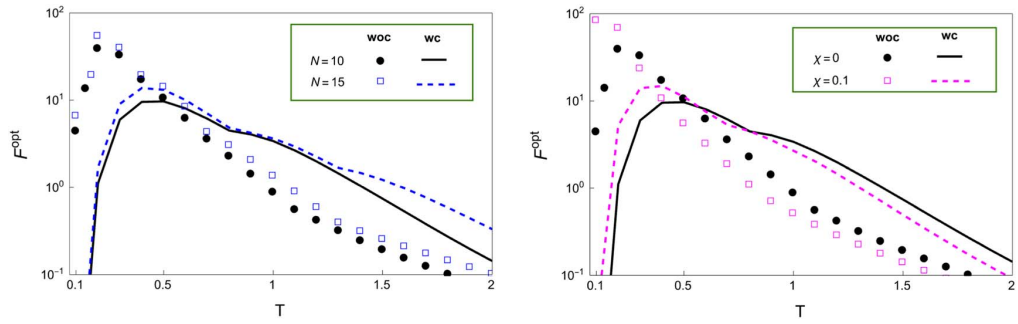

(a) Effect of no. of environmental spins **(b)** Effect of inter-spins interaction

Figure 4. Figures illustrate the behaviour of the F^{opt} estimating environment temperature with and without initial correlations. Plots in 4(a) show the effect of the number of environmental spins, $N = 10$ Vs $N = 15$, ignoring inter-spin interaction. 4(b) incorporates the effect of inter-spin interaction $\chi = 0.1$ while keeping $N = 10$ fixed. Both consider probe-environment coupling strength $g = 1$ and other probe-environment parameters are selfsame as in figure 2.

if somehow decoherence is prolonged, we can cast a large environment to avail higher accuracy. One possible way to lengthen the decoherence timescale is to use short repeated pulses (dynamical decoupling technique) [42]. We get similar results if inter-spin interaction is taken into account. It is important to note that by including inter-spin interaction, QFI slightly suppresses for both with or without the initial correlations cases. Finally, there is something common in both figures 4(a) and (b): the existence of a cross-over around $T = 0.5$. Before this point, QFI without initial correlations either with $N = 10$ or $N = 15$ is greater than that with correlations. However, after the cross-over point, we witness the converse effect. Thus, these plots give an overview of how one needs to choose a set of probe-environment parameters such that the accuracy is maximum.

4.3. Estimating probe-environment interaction strength

To estimate the probe-environment coupling strength, we use the same expression given in equations (9) and (10). All we need over here is to calculate the derivatives with-respect-to the coupling strength g. Then, as in the previous case, we compare the QFI obtained for both with and without initial correlations. First, we consider the case of high temperature, the results are shown in figure 5(a), where QFI is plotted against the interaction time, setting coupling strength to be fixed at $g = 0.01$. The red-solid curve denotes the results including correlations (wc) while black-dotted circles signify QFI disregarding correlations (woc). At least two points should be noted here. First, unlike the case of temperature estimation, here QFI keeps on increasing with time, suggesting that interaction time has to be prolonged for higher precision. Second, The overlap of the *woc*, and *wc* curves shows that correlations are not of any benefit. A similar trend persists in the stronger coupling figure 5(b), where can still see the overlaps. In both of these cases, we witness no appreciable quantitative difference between both with or without correlations. However, if we compare figures 5(a) and (b) with each other, we can clearly see how higher temperature and stronger coupling ($g = 0.5$) have sped up the decoherence time, as a result restricting us

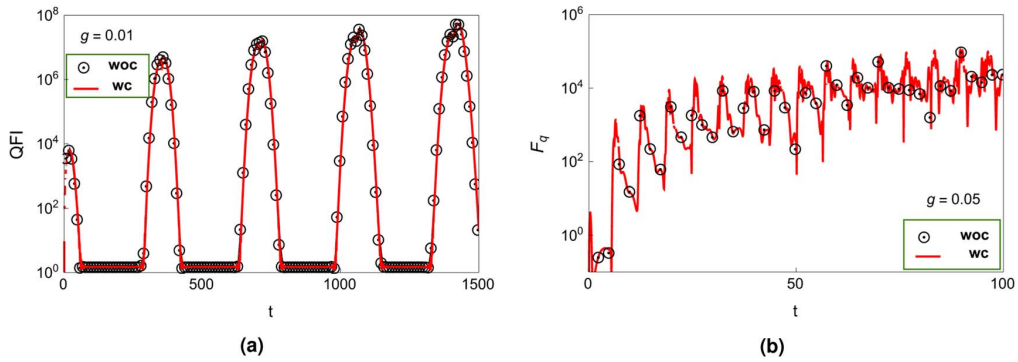

Figure 5. Figures illustrate the behavior of the QFI estimating coupling strengths $g = 0.01$ (left-hand plots) and $g = 0.5$ (right-hand plots) with and without initial correlations at $T = 5$. Other parameters are similar to figure 2.

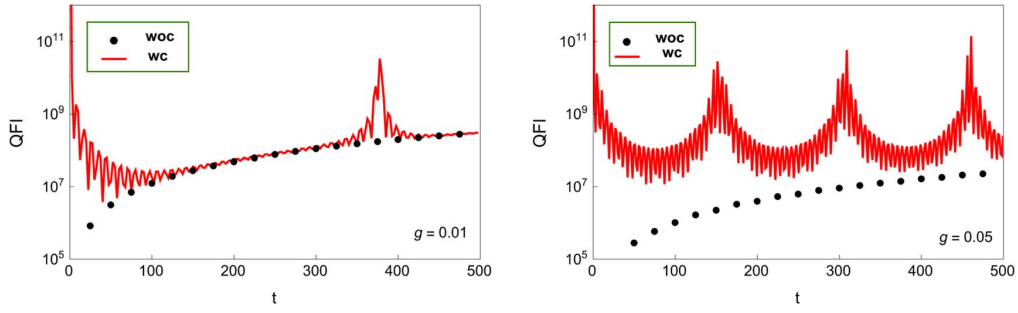

Figure 6. Same as figure 5 except $T = 0.1$ for both of the above figures.

to avail higher accuracy. Mathematically, it can be seen our QFI is directly linked with the decoherence rates Γ_c and Γ_u in equation (9) and equation (10) respectively.

Next, we move on to the low temperatures regime, where the correlation time is longer. The reason for this is obvious, since the sensitive quantum phase is no longer exposed to the thermal energies, hence quantumness can be preserved. Therefore, we expect a noticeable improvement in the precision if correlations are incorporated. Our forecast is illustrated in figure 6. Starting with the weak coupling ($g = 0.01$), we again see a continuous increase of QFI over time. However, we can now better differentiate between the *woc*, *wc* and curves. This difference is further amplified if we slightly tune up the coupling to $g = 0.05$. The ultimate goal of our work is blatant here once again as the lower bound has been lifted up by taking initial correlations into account.

In the case of coupling strength, Fisher information continuously increases with time. This behaviour is very interesting and in contrast with the case of temperature estimation. To dig out the cause of this peculiar behaviour, we show the curves in figure 7 for the derivatives of Ω, Γ, a_z with-respect-to temperature (in blue colour) and coupling strength (in red colour), as a function of time. In these plots, we chose the same set of probe-environment parameters. We notice that the derivatives w.r.t T are a bounded function of time whereas the derivatives w.r.t g diverge with time, making quantum Fisher information blow up as time goes on. This means that the Bloch vector components are highly oscillating function in a long time limit. Hence our probe becomes extremely sensitive to the coupling strength parameter g, and quantum Fisher information continuously increases with time

5. Discussion

Based on the estimation results presented in this paper, we deduce that the impact of initial probe-environment correlations is somehow advantageous in the estimation of environment parameters that is the environment's temperature and probe-environment coupling strength. In the temperature estimation, the precision does not significantly increase with the increase of coupling strength, but we noticeable improvement can be seen in the case of initial correlations. As we reduce the number of spins in the environment, QFI also seems to be

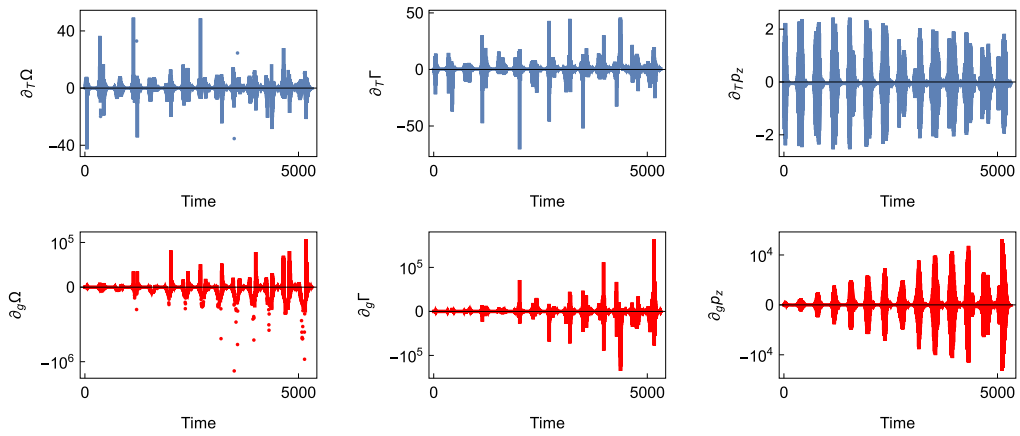

Figure 7. The behaviour of the derivatives of Ω, Γ, and a_z as a function of time for the case of temperature (blue) and coupling strength (red) estimation.

decreasing in both cases under consideration. A similar trend has been seen if the inter-spin interaction is taken into account. As the quantitative difference is not appreciable, thus ignoring the nearest neighbours' interaction is a reasonable assumption within the chosen set of probe-environment parameters. On the other hand, in the case of coupling strength estimation, our results show a continuous increase in the QFI no matter what correlations are present or not. Nevertheless, by incorporating correlations, one can still witness that the precision of the estimates increases by orders of magnitude, especially at low temperatures.

6. Appendix: Probe dynamics without initial correlations

Here we assume that our probe and its environment are initially in the separated state, that is, $\rho = \rho_S \otimes \rho_E$ whereby no quantum correlations are present. Now we prepare our probe's initial state 'up' along the x-axis via projective measurement. In such a case, we have

$$\rho_u(t) = \frac{1}{Z_E}\sum_N c_N U_N(t)|\varphi\rangle\langle\varphi| U_N^\dagger(t) = \frac{1}{2}\begin{pmatrix} 1 + a_z^u(t) & e^{-\Gamma_u(t)}e^{-i\Omega_u(t)} \\ e^{-\Gamma_u(t)}e^{i\Omega_u(t)} & 1 - a_z^u(t) \end{pmatrix}, \tag{11}$$

here we have $Z_E = \sum_N c_N$ whereas other time-dependent factors have already been defined in the main text of the paper. Thus, the evolution of the Bloch vector components can be written in general form as $a_i^u(t) = \Lambda_{ix}^u(t) a_i^u(0)$, with $i = x, y, z$, where

$$\Lambda_{xx}^u(t) = \sum_N \frac{c_N}{4Z_E\eta_N^2}\{\Delta^2 + \eta_N^2\cos(2\eta_N t)\};$$
$$\Lambda_{yx}^u(t) = \sum_N \frac{c_N \varepsilon_N}{2Z_E\eta_N}\sin(2\eta_N t);$$
$$\Lambda_{zx}^u(t) = \sum_N \frac{c_N \tilde{\epsilon}_N \Delta}{2Z_E\eta_N^2}\sin^2(\eta_N t)$$

igenvalues of equation (11) are $\rho_1^u(t) = \frac{1}{2}[1 + A_u(t)]$, $\rho_2^u(t) = \frac{1}{2}[1 - A_u(t)]$, with $A_u(t) = \sqrt{\{a_x^u(t)\}^2 + \{a_y^u(t)\}^2 + \{a_z^u(t)\}^2}$. The corresponding eigenvectors are

$$|v_1^u(t)\rangle = \sqrt{\frac{A_u(t) + a_z^u(t)}{2A_u(t)}}\,|\downarrow\rangle_z - e^{-i\Omega_u(t)}\sqrt{\frac{A_u(t) - a_z^u(t)}{2A_u(t)}}\,|\uparrow\rangle_z, \tag{12a}$$

$$|v_2^u(t)\rangle = \sqrt{\frac{A_u(t) - a_z^u(t)}{2A_u(t)}}\,|\downarrow\rangle_z + e^{-i\Omega_u(t)}\sqrt{\frac{A_u(t) + a_z^u(t)}{2A_u(t)}}\,|\uparrow\rangle_z. \tag{12b}$$

Acknowledgments

A R Mirza and J Al-Khalili are grateful for support under grant no. RN0491A from the John Templeton Foundation Trust. We also acknowledge useful discussions with Dr Adam Zaman Chaudhry and Dr Ahsan Nazir.

Data availability statement

All data that support the findings of this study are included within the article (and any supplementary files).

ORCID iDs

Ali Raza Mirza https://orcid.org/0000-0002-8532-7699

References

[1] Haroche S, Raimond J-M and Dowling J P 2014 Exploring the quantum: Atoms, cavities, and photons *Am. J. Phys.* **82** 86–7
[2] Schlosshauer M A 2007 *Decoherence: And the Quantum-to-classical Transition* (Springer Science & Business Media)
[3] Breuer H-P *et al* 2002 *The Theory of Open Quantum Systems* (Oxford University Press on Demand)
[4] Benedetti C, Buscemi F, Bordone P and Paris M G 2014 Quantum probes for the spectral properties of a classical environment *Phys. Rev.* A **89** 032114
[5] Mirza A R and Chaudhry A Z 2024 Improving the estimation of environment parameters via a two-qubit scheme *Sci. Rep.* **14** 6803
[6] Correa L A, Mehboudi M, Adesso G and Sanpera A 2015 Individual quantum probes for optimal thermometry *Phys. Rev. Lett.* **114** 220405
[7] Elliott T J and Johnson T H 2016 Nondestructive probing of means, variances, and correlations of ultracold-atomic-system densities via qubit impurities *Phys. Rev.* A **93** 043612
[8] Norris L M, Paz-Silva G A and Viola L 2016 Qubit noise spectroscopy for non-gaussian dephasing environments *Phys. Rev. Lett.* **116** 150503
[9] Tamascelli D, Benedetti C, Olivares S and Paris M G 2016 Characterization of qubit chains by feynman probes *Phys. Rev.* A **94** 042129
[10] Streif M, Buchleitner A, Jaksch D and Mur-Petit J 2016 Measuring correlations of cold-atom systems using multiple quantum probes *Phys. Rev.* A **94** 053634
[11] Benedetti C, Sehdaran F S, Zandi M H and Paris M G 2018 Quantum probes for the cutoff frequency of ohmic environments *Phys. Rev.* A **97** 012126
[12] Razavian S, Benedetti C, Bina M, Akbari-Kourbolagh Y and Paris M G 2019 Quantum thermometry by single-qubit dephasing *The European Physical Journal Plus* **134** 284
[13] Gebbia F *et al* 2020 Two-qubit quantum probes for the temperature of an ohmic environment *Phys. Rev.* A **101** 032112
[14] Wu W and Shi C 2020 Quantum parameter estimation in a dissipative environment *Phys. Rev.* A **102** 032607
[15] Tamascelli D, Benedetti C, Breuer H-P and Paris M G 2020 Quantum probing beyond pure dephasing *New J. Phys.* **22** 083027
[16] Gianani I *et al* 2020 Discrimination of thermal baths by single-qubit probes *Physical Review Research* **2** 033497
[17] Mirza A R 2023 Improving the understanding of the dynamics of open quantum systems arXiv:2402.10901
[18] Mirza A R, Zia M and Chaudhry A Z 2021 Master equation incorporating the system-environment correlations present in the joint equilibrium state *Phys. Rev.* A **104** 042205
[19] Morozov V, Mathey S and Röpke G 2012 Decoherence in an exactly solvable qubit model with initial qubit-environment correlations *Phys. Rev.* A **85** 022101
[20] Mirza A R, Jamil M N and Chaudhry A Z 2024 The role of initial system-environment correlations with a spin environment *Int. J. Mod. Phys.* B **38** 2450429
[21] Genoni M G, Olivares S and Paris M G 2011 Optical phase estimation in the presence of phase diffusion *Phys. Rev. Lett.* **106** 153603
[22] Spagnolo N *et al* 2012 Phase estimation via quantum interferometry for noisy detectors *Phys. Rev. Lett.* **108** 233602
[23] Pinel O, Jian P, Treps N, Fabre C and Braun D 2013 Quantum parameter estimation using general single-mode gaussian states *Phys. Rev.* A **88** 040102
[24] Chaudhry A Z 2014 Utilizing nitrogen-vacancy centers to measure oscillating magnetic fields *Phys. Rev.* A **90** 042104
[25] Chaudhry A Z 2015 Detecting the presence of weak magnetic fields using nitrogen-vacancy centers *Phys. Rev.* A **91** 062111
[26] Benedetti C and Paris M G 2014 Characterization of classical gaussian processes using quantum probes *Phys. Lett.* A **378** 2495–500
[27] Candeloro A *et al* 2021 Quantum probes for the characterization of nonlinear media *Entropy* **23** 1353
[28] Ciampini M A *et al* 2016 Quantum-enhanced multiparameter estimation in multiarm interferometers *Sci. Rep.* **6** 28881
[29] Uchiyama C and Aihara M 2010 Role of initial quantum correlation in transient linear response *Phys. Rev.* A **82** 044104
[30] Smirne A, Breuer H-P, Piilo J and Vacchini B 2010 Initial correlations in open-systems dynamics: The jaynes-cummings model *Phys. Rev.* A **82** 062114
[31] Dajka J and Łuczka J 2010 Distance growth of quantum states due to initial system-environment correlations *Phys. Rev.* A **82** 012341
[32] Chaudhry A Z and Gong J 2013 Amplification and suppression of system-bath-correlation effects in an open many-body system *Phys. Rev.* A **87** 012129
[33] Reina J H, Susa C E and Fanchini F F 2014 Extracting information from qubit-environment correlations *Sci. Rep.* **4** 1–7
[34] Chaudhry A Z and Gong J 2013 Role of initial system-environment correlations: A master equation approach *Phys. Rev.* A **88** 052107
[35] Chaudhry A Z and Gong J 2014 The effect of state preparation in a many-body system *Can. J. Chem.* **92** 119–27
[36] Zhang Y-J, Han W, Xia Y-J, Yu Y-M and Fan H 2015 Role of initial system-bath correlation on coherence trapping *Sci. Rep.* **5** 1–9
[37] Chen C-C and Goan H-S 2016 Effects of initial system-environment correlations on open-quantum-system dynamics and state preparation *Phys. Rev.* A **93** 032113
[38] De Vega I and Alonso D 2017 Dynamics of non-markovian open quantum systems *Rev. Mod. Phys.* **89** 015001

[39] Buser M, Cerrillo J, Schaller G and Cao J 2017 Initial system-environment correlations via the transfer-tensor method *Phys. Rev.* A **96** 062122
[40] Majeed M and Chaudhry A Z 2019 Effect of initial system-environment correlations with spin environments *Eur. Phys. J.* D **73** 1–11
[41] Zhang C and Gong B 2024 Improving the accuracies of estimating environment parameters via initial probe-environment correlations *Phys. Scr.* **99** 025101
[42] Ather H and Chaudhry A Z 2021 Improving the estimation of environment parameters via initial probe-environment correlations *Phys. Rev.* A **104** 012211